A Combined Experimental and Modelling Study on Solubility of Calcium Oxalate Monohydrate at Physiologically Relevant pH and Temperatures

Ibis, F.; Dhand, P.; Suleymanli, S.; van der Heijden, A.E.D.M.; Kramer, H.J.M.; Eral, H.B.

DOI
10.3390/cryst10100924

Publication date
2020

Document Version
Final published version

Published in
Crystals

crystals

MDPI

Article

A Combined Experimental and Modelling Study on Solubility of Calcium Oxalate Monohydrate at Physiologically Relevant pH and Temperatures

Fatma Ibis [1], Priya Dhand [1], Sanan Suleymanli [1], Antoine E. D. M. van der Heijden [1], Herman J. M. Kramer [1] and Huseyin Burak Eral [1,2,*]

[1] Intensified Reaction & Separation Systems, Process & Energy Department, Delft University of Technology, Leeghwaterstraat 39, 2628 CB Delft, The Netherlands; F.Ibis-1@tudelft.nl (F.I.); priya_dhand@hotmail.com (P.D.); che.suleymanli@gmail.com (S.S.); A.E.D.M.vanderHeijden@tudelft.nl (A.E.D.M.v.d.H.); H.J.M.Kramer@tudelft.nl (H.J.M.K.)

[2] Van't Hoff Laboratory for Physical and Colloid Chemistry, Debye Institute for Nanomaterials Science Utrecht University, 3584 CH Utrecht, The Netherlands

* Correspondence: H.B.Eral@tudelft.nl

Received: 31 August 2020; Accepted: 9 October 2020; Published: 12 October 2020

Abstract: Accurate Calcium Oxalate Monohydrate (COM) solubility measurements are essential for elucidating the physiochemical mechanism behind the formation of kidney stones, nephrolithiasis. Yet the reported solubility values of COM in ultrapure water, arguably the simplest solvent relevant for nephrolithiasis, vary significantly depending on implemented method. To address this variation, we present an experimental study of the solubility of COM validated by a model based on the Debye–Hückel theory describing the solution chemistry and the complex formation. We also carefully monitor potential pseudopolymorphic/hydrate transitions during the solubility measurements with in-situ and ex-situ methods. Our results indicate that the solubility of COM in ultrapure water is a weak function of temperature. However, the measured solubility varies significantly in buffer solutions across physiologically relevant pH values at body temperature. The proposed model explains observed trends as a combined effect of ionic strength, protonation reactions, and soluble complex formation. Moreover, it predicts solubility of COM in buffer solutions remarkably well using our measurements in ultrapure water as input, demonstrating the consistency of presented approach. The presented study parleying experiments and modelling provides a solid stepping stone to extend the physiochemical understanding of nephrolithiasis to more realistic solutions laden with biological complexity.

Keywords: kidney stone; nephrolithiasis; solubility of calcium oxalate monohydrate; temperature and pH effects on solubility of sparsely soluble salts; Debye–Hückel; whewellite

1. Introduction

Nephrolithiasis can be seen as the crystallization of inorganic salts and their consequent aggregation in the presence of biological complexity in the human kidney. This disease affects about 12% of the world population and its prevalence is increasing [1,2]. The driving force behind nucleation, the first step in formation of kidney stones, is the supersaturation of urine concerning the stone constituents such as calcium, oxalate, and phosphate ions [3,4]. Patient-specific information such as patient age, genetic effects, medical treatment history, fluid intake, diet habits, urine pH, and environmental conditions have also been reported as significant factors in formation of kidney stones [5–7]. To prevent kidney stone disease and its recurrence, first of all a better understanding of the underlying physiochemical mechanism of stone formation in the kidney is needed. Such an investigation should shed light on the

questions such as why some people under normal physiological conditions form kidney stones in the urinary tract, while others do not.

There are three main types of stones: Calcium oxalate, calcium phosphate, and uric acid [8–10]. Calcium oxalate (CaOx) comprises 80% of the kidney stones, which is found in the form of hydrates [11–14]. It occurs as dihydrate (weddellite) or monohydrate (whewellite) [5,6]. Calcium Oxalate Monohydrate (COM) is the most commonly seen and the most stable form with very low water solubility [5,9,15,16]. It is attributed mostly to idiopathic hypercalciuria. Hypercalciuria stones are caused due to a high calcium level in urine [5,17].

Urine is a waste product of our body consisting of a complex aqueous solution of urea, containing all kinds of organic and inorganic salts, soluble nitrogen products, and various biomolecules. The presence of these compounds influences the pH of the urine solution and has a strong influence on the crystallization of calcium oxalate, the main component of kidney stones [8]. Clinical studies indicated that pH values between 4.5 and 5.5 form the highest risk for forming kidney stones [8,18]. Even though the average pH of urine is 6.0, it can range between 4.0 and 8.0 [19]. Prediction of the crystallization behavior of COM crystals in such an environment therefore required precise knowledge on the influences of the composition and pH of the urine solution in the kidney on the solubility as well as on the nucleation and growth kinetics of these crystals. In this study, we concentrate on the solubility of COM while carefully monitoring the potential polymorphic transitions. The solubility of COM is reported to be strongly influenced by solution properties—the pH and ionic strength—emphasizing the presence of electrolytes, the speciation of the different ions as well as the formation of ionic pairs in the solution [20–22].

The solubility of calcium oxalate (CaOx) in pure water has been previously reported in the literature [23–27]. However, the stated values vary significantly as shown in Table 1. This large variation among reported values might be related to either the accuracy of the detection techniques used to determine the calcium or the oxalate concentrations, or different preparation methods used to create a saturated COM solution i.e., dissolution or precipitation, potentially resulting different polymorphic forms of COM. More importantly, standard deviation was not reported in most of reported measurements making it difficult to pinpoint the origin of this variation [23–29]. This inconsistency calls for a systematic experimental study comparing different methods.

Table 1. The solubility of CaOx in pure water at 25 °C. In reports provided below, hydrate form of dissolved CaOx has not been reported or characterized hence we can refer them as CaOx solubility unless hydrate form is explicitly mentioned.

Authors	Year	Solubility 10^{-4} [M]	Measurements Method
Gutzow et al. [26]	1993	0.57	Atomic absorption spectrometry
Molzon [23]	1976	1.329	Dielectric constant measurements
McComas et al. [24]	1942	0.455	Titration
Shehyn and Pall [25]	1940	0.60	Titration
Hammarsten [28]	1929	0.466	Titration
Herz et al. [27]	1903	2.33	Titration
Singh et al. [20]	1989	0.564	Ion Chromatography

More recent studies have focused on solubilities in more physiologically relevant solutions for formation of kidney stones, such as urine-like or artificial urine solutions. Those studies revealed that background electrolytes like NaCl [22,30,31], lead to an increased solubility, which has been

attributed to the influence of the electrolyte solution on the activity coefficient of the Ca^{2+} and $C_2O_4^{2-}$ ions [22,31]. In addition, it was shown that the pH of the solution affects the speciation of the different components and thus the formation of ionic pair complexes of calcium and oxalate ions. As such the pH can have a strong influence on the solubility of COM and the crystallization kinetics [22,30–32]. In more complex solutions, the ratio of Ca and oxalate ions can vary considerably, stressing the need to express the solubility in terms of the thermodynamic solubility product [21,22,33]. Streit et al. compared their own and literature values of the thermodynamic solubility product K_{sp} and reported a value of K_{sp} of 1.7×10^{-9} $mol^2 \cdot L^{-2}$ for COM at 25 °C [22]. However, he also noted an inconsistency between solubility measurements using atomic absorption spectroscopy and those using the calcium electrode measurements.

The interpretation of solubility experiments in more complex solutions requires precise estimation of the composition effects on the activity of the relevant components. Besides, a detailed analysis of the possible reactions and complex formation is essential to understand the behavior of these solutions as a function of pH and composition. A number of attempts have been made to interpret solubility and crystallization results in different solutions with varying complexity ranging from the water with background electrolytes up to urine samples of stone-forming patients [22,24,30,31,33–35]. However, the previous studies did not consistently cover physiologically relevant pH and temperature ranges while considering composition effects on the activity of the relevant components. The aforementioned variation in reported the solubility measurements of COM in ultrapure water and the lack of a systematic study on pH dependency of this solubility hampers modeling efforts.

This work describes a coupled experimental and modeling study on the solubility of the calcium oxalate monohydrate as a function of temperature and pH, monitoring the polymorphic form of the crystalline phase to rule out possible transformations into other hydrates of CaOx. To select the most appropriate analytical method to measure the solubility of this sparsely soluble compound, we first conducted a comparative study of the solubility measurements using a number of analytical methods as a function of temperature. Once the most appropriate analytical method was identified, we proceeded to measure the solubility of COM as a function of pH in buffer solutions at body temperature. Moreover, we developed a solution chemistry model based on Davies extension of Debye-Hückel theory and compared the theoretical predictions to experimental results. The influence of the pH on the solubility of COM is quantified at body temperature in two different buffer solutions, i.e., citric acid-disodium phosphate and glycine-sodium hydroxide chosen to stabilize the pH between 3.2–7.55 and from 9.0 to 10.6, respectively. Finally, we used the developed a solution chemistry model to elucidate the effects of the process conditions, ionic strength, and complex formation on the solubility of COM [36]. The proposed model coupled with the Van't Hoff equation enabled the calculation of the solubility product of COM, K_{sp} from the solubility measurements as a function of temperature. These K_{sp} values implemented in the developed model provided excellent predictions for the soluble Ca^{2+} ion concentration measurements at different pH values in two different buffer solutions kept at body temperature. This excellent prediction without fudge factors highlight the consistency of the presented study parleying experiments with modeling. We believe our combined study provides a solid stepping stone to extend the developed physiochemical understanding to more realistic and complex solutions relevant for nephrolithiasis.

2. Materials and Methods

As mentioned previously, solubility measurements of sparsely separated compounds are challenging due to minute amounts of material involved. To identify the ideal measurement method for this task, we systematically tested the following methods: (i) gravimetric method to isolate non-volatile components saturated COM, (ii) the turbidity-based solubility method using multiple reactor systems Crystal16 and Crystalline (Avantium Technologies, Amsterdam, The Netherlands), (iii) UV-VIS Spectrophotometry, (iv) Focused Beam Reflectance Measurement (FBRM D600L, Mettler Toledo, Columbus, OH, USA), (v) in situ Infrared spectroscopy (ReactIR iC10 Mettler Toledo,

Columbus, OH, USA) coupled to temperature-controlled and well-mixed vessel, EasyMax [37–39], (vi) titration, (vii) Inductively Coupled Plasma Optical Emission Spectroscopy (ICP-OES, SPECTRO Analytical Instruments, Kleve, Germany), and (viii) Inductively Coupled Plasma Mass Spectroscopy (ICP-MS, Analytik Jena AG, Jena, Germany). The tested methods are illustrated in Figure 1. For the sake of completeness, we provide here a list of all tested methods yet only titration, ICP-OES, and ICP-MS produced consistent results and are presented in Figures 2 and 3. The detailed procedures and discussion for other methods are provided in Supplementary Materials. The experimental section is organized as follows: First, the method for preparing an equilibrated suspension is described in Sections 2.1 and 2.2, followed by description of analytical detection methods in Sections 2.3–2.5 and finally pseudopolymorphic/hydrate characterization of excess COM in-situ and ex-situ in Section 2.6.

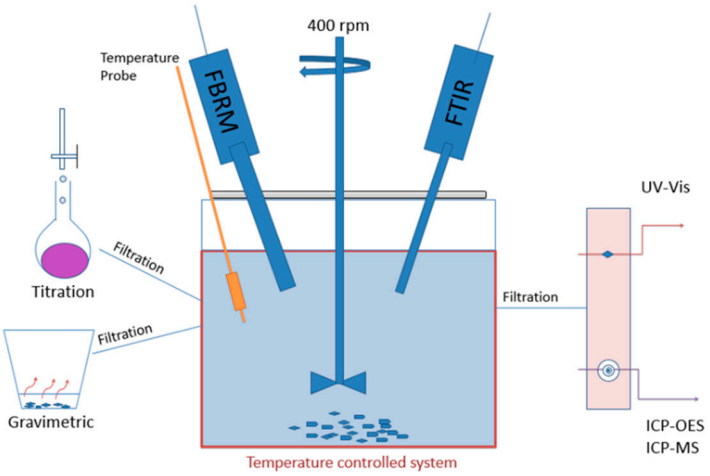

Figure 1. Schematic illustration of isothermal solubility experiments. A suspension of excess Calcium Oxalate Monohydrate (COM) crystals in ultrapure water or a buffer solution was brought in equilibrium at designated temperature and pH values. The suspension is filtered to isolate the saturated solution from crystals at fixed temperature. The saturated solution is diluted at the same temperature to avoid crystallization. The calcium and oxalate ion concentrations in filtered saturated solution are analyzed with the following methods, commonly used for measuring solubility of highly insoluble compounds in literature (from the left to right); gravimetric, titration, Focused Beam Reflectance Measurement (FBRM), FTIR, UV-Vis, Inductively Coupled Plasma Optical Emission Spectroscopy (ICP-OES), and Inductively Coupled Plasma Mass Spectroscopy (ICP-MS). The pseudopolymorphic/hydrate form of the excess solute is quantified prior to and at the end of experiments via in-situ and ex-situ methods.

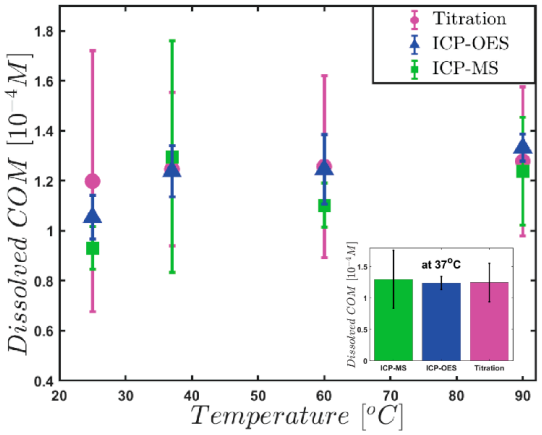

Figure 2. Measured dissolved COM in ultrapure water as a function of temperature for the three analysis methods. Average values and their standard deviations are given for titration (magenta circles), ICP-OES (blue triangles), and ICP-MS (green squares). The error bars denote the standard deviation of independent repetitions. The inset shows the solubilities measured at body temperature.

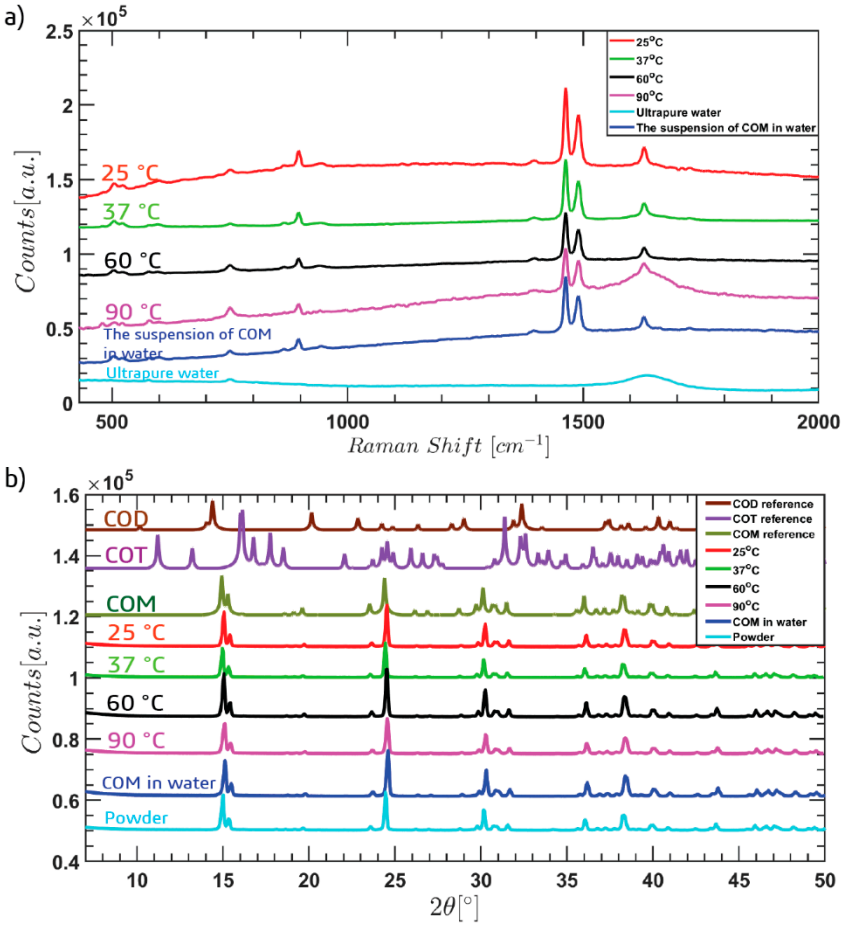

Figure 3. Characterization of suspended crystals in ultrapure water at different temperatures for ICP-OES experiments. (**a**) The results of six Raman measurements, 25 °C; red, 37 °C; green, 60 °C; black; 90 °C; magenta; the suspension of COM in water prior to experiment; blue, ultrapure water; cyan. (**b**) The results of nine XRD measurements. 25 °C; red, 37 °C; green, 60 °C; black; 90 °C; magenta, COM suspension filtered and dried at room temperature denoted as "COM in water"; blue, Powder (COM powder from supplier); cyan, COM reference; dark green, Calcium Oxalate Dihydrate (COD) reference; brown and Calcium Oxalate Trihydrate (COT) reference; purple.

2.1. Preparation of Equilibrated Suspensions for ICP-OES and ICP-MS

In all of the experiments described above, an excess amount of calcium oxalate monohydrate ($CaC_2O_4{\cdot}H_2O$, Sigma-Aldrich, CAS563-72-4, St. Louis, MO, USA) crystals are brought in equilibrium with an aqueous solution (pure water (ELGA PURELAB, Resistivity: 18.2 MΩ·cm at 23.6 °C) or a buffer solution at a given temperature in a well-mixed, temperature-controlled vessel (Figure 1). Once the equilibrium is established, an aliquot of the saturated solution carrying calcium and oxalate ions in equilibrium with COM in crystal phase is filtered, diluted with pure solvent (either ultrapure water or buffer solution), and analyzed. We used EasyMax 102 (Mettler Toledo), a jacketed vessel, to control the temperature and stirring rate (400 rpm). Twenty milligrams of COM crystals were suspended in 100 mL ultrapure water or 100 mL buffer solution and allowed to equilibrate at targeted temperature and pH for one hour. To ensure that thermodynamic equilibrium is reached, we conducted experiments at different equilibration times, namely 30 min, one hour, two hours, and four hours. The measured solubility values did not change significantly (<1%) after one hour, hence we chose one hour as our canonical equilibration time. For temperature dependence of solubility measurements, COM crystal dispersed in ultrapure water were rigorously mixed, and the resulting suspension was allowed to equilibrate at 25 °C, 37 °C, 60 °C, and 90 °C. For measuring the pH dependence of solubility of COM,

the suspension was allowed to equilibrate in buffer solutions with set pH values 3.2, 5.36, 6.0, 7.55, 9.0, and 10.6, respectively, at 37 °C. After the solution was kept at the desired temperature and pH to reach solid-liquid equilibrium, the stirrer was stopped, and samples were taken from the top portion of the vessel.

Aliquoting of the saturated solution is performed in three steps: Pipetting, filtration, and dilution. When the stirrer of Easymax is stopped, the crystals are allowed to sediment and 1 mL solution is taken with a 1 mL pipette. The equilibrated solution is filtered with syringe and filter (Whatman, 0.22 µm pore diameter) kept at the same temperature as the suspension in a separate oven. The samples were 10× diluted into 10 mL volumes with pure ultrapure water or buffer solution kept at the same temperature as the suspension to avoid precipitation. Ten milliliters of samples are needed for the analysis with ICP-OES and ICP-MS. For each experimental condition, the identical samples are divided into two groups for ICP-OES and ICP-MS analysis.

A buffer solution is chosen considering the possibilities of the binding capacity of calcium with other compounds present in the buffer solution. The most convenient options are citric acid-disodium phosphate for the lower pH range and glycine-sodium hydroxide for the higher pH range. The buffer solutions are prepared in 1000 mL Erlenmeyer and placed in the ultrasonic bath for 10 min. Afterward, the buffer solution is placed on the magnetic stirrer at 37 °C and 400 rpm. The buffer solutions used in pH dependent solubility measurements are given in Table 2.

Table 2. Used buffer solutions for different pH values [40,41].

pH	Mixing of Buffer Solutions
3.2, 5.36, 6.0, 7.55	Citric Acid ($C_6H_8O_7$) (Merck, CAS: 77-92-9) Disodium phosphate (Na_2HPO_4) (Sigma-Aldrich, CAS: 7558-79-4)
9.0, 10.6	Sodium hydroxide (NaOH) (Sigma-Aldrich, CAS: 7558-79-4) Glycine ($C_2H_5NO_2$) (Sigma-Aldrich, CAS: 1310-73-2)

2.2. Preparation of Equilibrated Suspensions for Titration

This procedure is analogous to preparation of equilibrated suspensions for ICP-OES and ICP-MS yet certain details such as amount of suspension and method to maintain the solution constant temperature are adapted for the requirements of titration experiment. Ten milligrams of COM are mixed with 50 mL of ultrapure water in a beaker. The suspension is equilibrated on a hot plate at the targeted temperature at a stirring rate of 400 rpm for three hours. A longer equilibration time, three hours instead of one hour used in ICP-OES and ICP-MS measurements, was chosen to account for the less stringent temperature control of the hot plate compared jacketed EasyMax 102 reactor.

2.3. Inductively Coupled Plasma-Optical Emission Spectrometry (ICP-OES)

The filtrate of the COM suspensions equilibrated at different temperature and pH values were analyzed at three possible calcium emission lines at 317.9, 393.4, and 396.3 nm (See Supplementary Materials). The measurements conducted at all three wavelengths quantitatively show the same trend yet the emission line of 317.9 nm gave the smallest standard deviation. This situation is also observed in the literature and attributed to interference from other ions present [42–44]. The experiments were conducted with more than seven samples for each temperature, 25 °C, 37 °C, 60 °C, and 90 °C. At body temperature condition, nine replicate samples were analyzed for each pH; namely, 3.2, 5.36, 7.55, 9.0, and 10.6 and five replicate samples were analyzed for pH 6.0 [41,45].

2.4. Inductively Coupled Plasma-Mass-Spectrometry (ICP-MS)

We prepared at least seven replicates for each temperature and nine samples for each pH. The filtrates of each sample are analyzed with ICP-MS. While ICP-OES can detect ppm level, ICP-MS can detect parts per billion (ppb level) [37] as ICP-MS measures a mass-to-charge ratio, an intrinsically more sensitive approach compared to optical emission used in ICP-OES [39].

2.5. Titration

After filtration, the COM filtrate was mixed (1:10 volume-based) with a 9.5% Sulphuric acid solution (Merck, CAS: 7664-93-9). Triplicate experiments were performed at 25 °C, 37 °C, 60 °C and 90 °C. In the titration reactions, filtrated samples were titrated with a 7×10^{-4} M Potassium Permanganate (MnO_4^-) solution until the color change was observed. The concentration of oxalate was calculated via the amount of titrated permanganate.

2.6. Pseudopolymorphic/Hydrate Form Characterization of Excess COM Crystals in Equilibrated Suspension

To check whether COM crystals in suspension transformed to other calcium oxalate hydrates during solubility measurements at experimental temperature and pHs, we quantified the polymorphic form of the crystals prior to and after equilibration via in-situ via Raman scattering, and ex-situ methods via powder X-ray diffraction, PXRD. Due to low solubility of COM, we repeated the procedure for preparation of equilibrated suspensions described in Section 2.1 10 times to get sufficient amount of COM crystals to employ Raman and X-ray diffraction detection (at different temperatures; 25 °C, 37 °C, 60 °C, 90 °C, at each pH values; 3.2, 5.36, 6.0, 7.55, 9.0, 10.6, and additionally COM suspension in ultrapure water referred to as no treatment). The suspensions were left undisturbed for one hour to allow the crystals to sediment. For in-situ Raman measurements, the sediment is decanted, and the concentrated suspension were analyzed with a Raman probe (Kaiser Optical Systems) immersed in suspension. For X-ray diffraction analysis, the crystals were isolated by filtration with 0.45-µm pore size filter (Whatman® membrane filters nylon), then washed with ultrapure water three times and dried to avoid unwanted co-crystallization of buffer constituents, crystal attrition, or agglomeration. The washed crystals were kept at room temperature to dried for two days prior to PXRD experiments. Approximately 150 milligrams of crystals were collected for each experimental condition. PXRD experiments were performed with these crystals placed on a silicon holder with a powder X-ray diffractometer (Bruker, Cu Ka1, k = 1.5406 A°). The acquired spectra were compared to reference spectra of COM, Calcium Oxalate Dihydrate (COD), and Calcium Oxalate Trihydrate (COT) in Cambridge Crystallographic Data Centre (CCDC). The plotted PXRD patterns taken from the CCDC software tool are the following COM (CALOXM03), COD (CAOXAL), and COT (ZZZUOQ01).

A model was developed to describe the dissolution of COM in ultrapure water based on the solution chemistry. The proposed model considers the protonation reactions of the oxalate ions in the solution and also the formation of the ion pairs between Ca^{2+} and $C_2O_4^{2-}$ ions forming soluble complexes of CaC_2O_4 [30,46]. Equations (1) and (2) describe the equilibrium of the protonation reaction of $HC_2O_4^-$ and of $C_2O_4^{2-}$, respectively, using their temperature dependent association constants.

$$K_{H_2C_2O_4} = \frac{a_{H_2C_2O_4}}{a_{H^+} a_{HC_2O_4^-}} \quad (1)$$

$$K_{HC_2O_4^-} = \frac{a_{HC_2O_4^-}}{a_{H^+} a_{C_2O_4^{2-}}} \quad (2)$$

In these equations, a_i represents the activity of the species i, which is by definition equal to the product of the concentration in solution multiplied with the activity coefficient. In electrolyte solutions, part of the Ca^{2+} ions and $C_2O_4^{2-}$ ions will be bound in so-called soluble ion pair complexes and are as

such not available for crystallization. At Equation (3), the amount of such a complex can be described using an association constant.

$$K_{CaC_2O_4} = \frac{a_{CaC_2O_4,(aq)}}{a_{Ca^+} a_{C_2O_4^{2-}}} \quad (3)$$

where CaC_2O_4 (aq) represents the ion pair or the aqueous form of CaC_2O_4. The presence of ion pair complexes can decrease the amount of free Ca^{2+} and ${C_2O_4}^{2-}$ ions in the solution and will thus affect the solubility of COM [22,30,31]. The solubility product of COM as reported by Nancollas and Gardner [46] is given in Equation (4).

$$K_{sp} = a_{Ca^{2+}} a_{{C_2O_4}^{2-}} \quad (4)$$

The solubility product of COM, K_{sp} is again assumed to be a temperature dependent constant. The temperature dependence of the equilibrium constants or solubility product, $K(T)$ is related to the enthalpy of the reaction using the Van't Hoff equation given below.

$$\ln\left(\frac{K(T)}{K_0}\right) = -\frac{\Delta H_R}{R}\left(\frac{1}{T} - \frac{1}{T_0}\right) \quad (5)$$

where $K_0 = K(T_0)$ is the value of the reaction or stabilization constant at standard conditions at 25 °C, ΔH_R [Jmol^{-1}] is the enthalpy of the reaction, R [Jmol^{-1}·K^{-1}] the gas constant, and T and T_0 [K] the actual and the standard temperature, respectively.

The values used for the different equilibrium constants and those for the enthalpy change of reaction are given in Table 3. In case ΔH_R was not given and temperature dependent K values were available, those values were fitted using the Van't Hoff equation estimating the parameters K_0 and T. The ΔH_R was assumed to be zero otherwise. The presence of a dicalcium oxalate complex (${Ca_2C_2O_4}^{2+}$) is also mentioned by some authors, but formation of this complex is generally assumed to be negligible in solubility experiments with low and stoichiometric Calcium and Oxalate concentrations [32,33]. Unfortunately, the reported K_{sp} values are not very consistent, which leads to a large discrepancy between experimental measured and simulated solubility values, as will be discussed later in detail.

Table 3. Associations constants K_0, solubility products of COM, and enthalpy of reaction of the given reactions from literate and the estimated values of $K_{sp,0}$ and ΔH_R of COM in this study. Estimated values are calculated using the temperature dependent solubility data of COM in ultrapure water given in Figure 4 using the proposed model.

Parameters	Reaction	Source	$K_0/K_{sp,0}$	ΔH_R [kJmol^{-1}]
$K_{H_2C_2O_4}$	$H_2C_2O_4 \rightleftarrows H^+ + HC_2O_4^-$	[33]	18.17 [L·mol^{-1}]	3.2
$K_{HC_2O_4^-}$	$HC_2O_4^- \rightleftarrows H^+ + C_2O_4^{2-}$	[33]	18,450 [L·mol^{-1}]	8.32
$K_{CaC_2O_4}$	$CaC_2O_4 \rightleftarrows Ca^{2+} + C_2O_4^{2-}$	[47]	2746 [L·mol^{-1}]	0
K_{sp}	$Ca^{2+} + C_2O_4^{2-} \rightleftarrows CaC_2O_4 \cdot H_2O$	[22]	1.7×10^{-9} [mol^2 L^{-2}]	17.9
Estimated K_{sp}	$Ca^{2+} + C_2O_4^{2-} \rightleftarrows CaC_2O_4 \cdot H_2O$	This study	6.7×10^{-9} [mol^2 L^{-2}]	5.5

The activity coefficients, γ_i in the model are estimated using the Davis extension of the Debye–Hückel theory [3] in which the activity coefficients of the different ions are directly related to the ionic strength of the solution I, and the charge of the ions, z_i

$$\log(\gamma_i) = -Az_i^2\left[\frac{\sqrt{I}}{1+\sqrt{I}} - 0.3I\right] \quad (6)$$

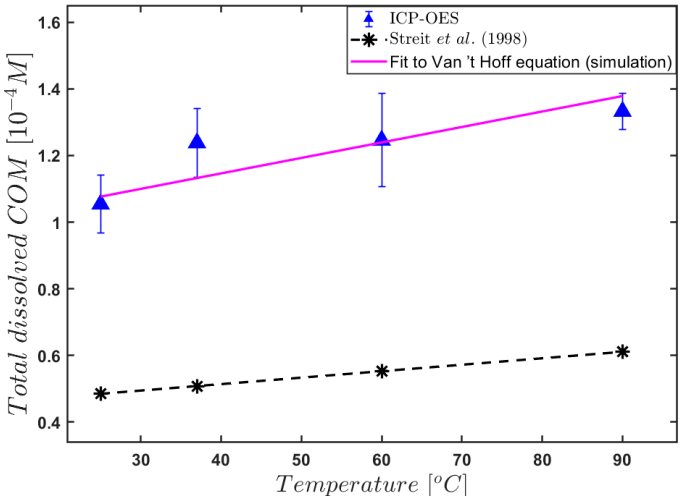

Figure 4. Total dissolved COM in ultrapure water measured by ICP-OES as a function of temperature (blue triangles). Simulated values using the K_{sp} values of Streit et al. [22] (black stars) and the fit of the ICP-OES results with the simulated total soluble Ca concentration after estimation of $K_{sp,0}$ and ΔH_R using the Van't Hoff equation (solid magenta line).

Here, A is a temperature dependent constant around 0.5 [33,48], and I is the ionic strength of the solution defined as:

$$I = -0.5 \sum_{i=1}^{N_{species}} c_i z_i^2 \tag{7}$$

where, c_i is the molar concentration of the ions and, z_i the charge of these ions. In order to simulate the solubility experiments in ultrapure water at different temperatures, the model calculates the concentrations of the possible species shown in Table 3 at the given conditions. For the COM water system, the concentration of the seven possible components, H^+, Ca^{2+} $C_2O_4{}^{2-}$, $HC_2O_4{}^-$, $H_2C_2O_4{}^{2-}$, $CaC_2O_{4\cdot aq}$, and COM are calculated using the material balances for oxalate, calcium, the charge balance, and Equations (1)–(4), while the relation between concentration and activities of the different species is described by the activity coefficients given by Equations (6) and (7). These equations are solved simultaneously using the Matlab function fsolve.

To simulate the experiments at different pH's in the buffer solutions, the approach is similar. However, the equilibrium between the protonation/de-protonation reactions of the acid species of the buffer solution, again described by an association constant, are considered as well.

As an example, for the citric acid (Cit), the four species Cit^{3-}, $HCit^{2-}$, H_2Cit^-, and H_3Cit are, at equilibrium, related by the following three equations:

$$K_{H_3Cit} = \frac{a_{H_3Cit}}{a_{H^+} a_{H_2Cit^-}} \tag{8}$$

$$K_{H_2Cit^-} = \frac{a_{H_2Cit^-}}{a_{H^+} a_{HCit^{2-}}} \tag{9}$$

$$K_{HCit^{2-}} = \frac{a_{HCit^{2-}}}{a_{H^+} a_{Cit^{3-}}} \tag{10}$$

where Cit^{3-} represents the fully deprotonated citric acid ion. The temperature dependence of the association constant is again described by the Van't Hoff equation (Equation (5)). Besides the protonation reactions, complexation reactions of the citric acid species with anions in the solution are considered. According to literature, the following complexes are relevant, $CaCit^-$, CaHCit, and $NaCit^{2-}$ [22,33,47]. For the phosphate and glycine species, similar protonation reactions can be formulated. Relevant

complexes for the phosphate and glycine ions that are considered in the program are $CaHPO_4$, $CaPO_4^-$, $NaPO_4^{2-}$ and $CaGly^+$. The values for the standard values of the association constants for the de-protonation and the complexation reactions and the ΔH_R values were taken from the literature [47,49,50] and are given in Supplementary Materials.

3. Results and Discussion

The temperature-dependent solubility of COM is determined in, ultrapure water. The solubility experiments were performed with the three methods described in the experimental section to find the most suitable method for this sparsely soluble salt (Figure 1). Titration, ICP-OES, and ICP-MS gave the most consistent results hence discussed in the main text. The rest of the methods are detailed in the supporting information.

First of all, we have to realize that using the titration method, the total oxalate concentration, including the free $C_2O_4^{2-}$ ions, the protonated species of the oxalate, and the oxalate in the CaOx complexes, is determined. In contrast, the total Calcium (free and complexed Calcium) concentration is determined in ICP-OES and ICP-MS methods. However, the total dissolved Calcium or Oxalate ion concentrations are not simply equal to the solubility of COM. The solubility of COM is defined as the square root of the solubility product, K_{sp}, which is equal to the product of the activities of free Ca^{2+} and $C_2O_4^{2-}$ ions as defined in Equation (4). The experimental results are thus expressed either as the total dissolved Ca concentration, the total dissolved oxalate concentration, or the total dissolved COM, which should be the same for these simple dissolution experiments in water due to stoichiometry. To determine the solubility product K_{sp}, however the activities of the ions should be estimated as well as the contribution of the protonated forms of the oxalate species and of the ion pair complexes, which is done using the model after validation.

In Table 4, the results of the solubility experiments are given for the three methods at four different temperatures. The results show a reasonable agreement in terms of the mean values for all methods. However, sizeable differences are found in the standard deviations of the different methods. Especially the titration method shows large standard deviations in Table 4. This is even better illustrated in Figure 2 and its inset, showing the temperature dependent solubilities measured with the three methods, including the standard deviations of the measurements. The error bars denoting the standard deviation of the ICP-OES measurements are distinctly smaller than those of the ICP-MS and the titration method, indicating that ICP-OES is the most suitable detection method for measuring the solubility of COM among the tested alternatives. Therefore, we use this technique in the remainder of this study as the standard measurement technique.

Table 4. The results of solubility of COM measurements in ultrapure water as a function of the temperature. The reported results are shown as the mean total ion concentration along with the standard deviations, σ.

Temperature (°C)	Titration [10^{-4} M]		ICP-OES [10^{-4} M]		ICP-MS [10^{-4} M]	
	$[C_2O_4^{2-}]_{tot}$	σ	$[Ca^{2+}]_{tot}$	σ	$[Ca^{2+}]_{tot}$	σ
25	1.198	0.521	1.054	0.087	0.931	0.086
37	1.244	0.307	1.238	0.103	1.296	0.463
60	1.258	0.378	1.246	0.140	1.102	0.089
90	1.279	0.290	1.332	0.055	1.238	0.216

The large standard deviations observed with the titration method might be due to manual nature of titration method where the experimentalist measures the titrated volume by judging color change by eye. In addition, saturated solution preparation for titration experiments were conducted with a beaker placed on a hot-plate. We suspect that hot-plate used in titration is less accurate in controlling the temperature compared to automated EasyMax 102 (Mettler Toledo, Columbus, OH, USA) used in saturated solution preparation for ICP-MS and ICP-OES. The larger variation observed with ICP-MS

compared to those of the ICP-OES were more of a surprise as in general the ICP-MS can detect elements down to ppb levels [37]. However, in the detection of calcium ions in the mass spectrometer, there is an overlap between the calcium and argon, which have similar molar masses. Due to the overlap with argon we could not use the normal calcium peak but were forced to measure the Calcium isotope, Ca-44, which, however, is much weaker leading to much higher uncertainties.

The measured values of the total dissolved Calcium concentration at room temperature in this study are generally high compared to the literature values (see Tables 1 and 4) with the exception of the dielectric measurements of Molzon [23] and titration experiments by Herz et al. [27]. Yet it is difficult to pinpoint the origin of this difference as most studies do not report a standard deviation [23–27]. Based on the hands-on experience from our measurements, we can only speculate on the origin of this variation. First of all, measurements of sparsely soluble salts are a challenge due to small amounts of material involved that are difficult to weigh accurately. Moreover, techniques requiring visual inspection such as manual titration are subject to human errors hence large standard deviations are expected. We observed standard deviation to vary between 0.3 to 0.5 $\times$ 10^{-4} M in our titration experiments, if we were to speculate similar standard deviations for four out of seven reported values in Table 1, the error bars between our measurements and these experiments will overlap for all but one report. In addition to detection method, the saturated solution preparation can also play a role in this variation between measured and reported values. For instance, saturated solution preparation methods such as rapid precipitation at high supersaturations are susceptible to impurity incorporation to crystals. This may result in impurity doped or coated crystals that dissolve slower than pure crystals. Such slow dissolution kinetics may lead to preparation of undersaturated solutions as opposed to saturated solutions. Also, high supersaturations created in the rapid precipitation approach can lead to crystallization of other hydrates (Calcium Oxalate Dihydrate (COD) or Calcium Oxalate Trihydrate (COT)) that have different solubilities. Finally, we characterize the pseudopolymorph/hydrate form of the raw material prior and right after solubility measurements (Figure 3), this characterization step is essential in dissolution measurements of compounds showing multiple phases or hydrates [51]. If the starting material is not pure COM but contains other hydrates, the measured solubility values will be influenced.

Moreover, the discussion in literature on ideal titration procedure is far from settled. The reported titration experiments in Table 1 vary in terms of sample preparation and various authors criticized each other's procedure. Richards et al. have studied calcium oxalate solubility [52] and their method was to treat hot and slightly acid solution of calcium chloride with an excess of oxalic acid. After neutralization, the solution was made distinctly ammoniacal by adding a large excess of ammonium oxalate. They found the solubility of COM as 0.531 $\times$ 10^{-4} M. Hall has criticized that Richards' study due to presence of "large excess of ammonium oxalate" [53], which could make the calcium oxalate less soluble in accordance with the solubility product principle and the common ion effect. This common ion effect along with our speculations on impurity incorporation and potential phase transitions [51] may explain the difference between the reported titration experiments in Table 1 and our measurements.

Shehyn and Pall have found solubility of COM in pure water as 0.646 $\times$ 10^{-4} M at 30 °C and 1.132 $\times$ 10^{-4} M at 95 °C [25]. Interestingly, their solubility value at 95 °C is quite similar to our results at 90 °C. More recently, Streit et al. reported solubility of COM in NaCl solutions of low concentrations [22]. They reported averaged solubilities of 0.78 $\times$ 10^{-4} at 25 °C and 0.98 $\times$ 10^{-4} at 37 °C, which are lower than our values but larger that most titration experiments in literature. The authors reported however a discrepancy between two methods utilized, i.e., Atomic Absorption Spectroscopy and a Ca selective electrode, which could not be explained by the modelled amount of $CaC_2O_4^{2-}$ ion pair complex formed. With increasing temperatures, the solubility of calcium was found to increases only slightly in our experiments in agreement with earlier results [30,32,50].

To ensure that solution pH did not change during solubility measurements at different temperatures, we measured the pH of COM solution in ultrapure water at each temperature shown in Figure 2 via

IDS pH electrode (pH-meter 914 pH/Conductometer Metrohm). It was found that the dissolution of COM has no significant effect on the pH of the solution in all measurements.

To quantify the pseudopolymorph/hydrate form of excess crystals, we performed Raman and PXRD measurements of our samples before and after the experiments. Figure 3a shows Raman spectra of crystals suspended in ultrapure water during isothermal dissolution experiment at different temperatures. In addition, Figure 3a contains Raman spectra of ultrapure water (without suspended crystals) and of suspended COM crystals as purchased from the manufacturer prior to dissolution experiment denoted as "COM suspended in water".

The characteristic COM Raman bands were observed in Figure 3a at 504, 508 (O–C–O), 897 (C–C), 1463, 1490 (C–O), and 1629 (C–O) cm^{-1} [54–56]. These shared peaks evident in four different temperatures and "The suspension of COM in water" spectra imply that the pseudopolymorphic/hydrate form of excess COM crystals did not change throughout dissolution experiments, even at highest temperature 90 °C. In addition to in-situ Raman measurements, we performed ex-situ PXRD measurements where the excess crystals are filtered, washed, and dried for diffraction measurements. Figure 3b provides PXRD spectra of excess crystals after dissolution experiments at four different temperatures along with reference spectra of three calcium oxalate phases from CCDC database, namely Calcium Oxalate Monohydrate (COM), Calcium Oxalate Dihydrate (COD), or Calcium Oxalate Trihydrate (COT) [57]. The PXRD peaks of COM reference match with the spectra from different temperatures as well as the PXRD spectra of COM crystals as purchased from supplier referred as "Powder". In line with Raman results in Figure 3a, this results points out that the polymorphic form of COM did not change throughout the dissolution measurements. Moreover, we checked rather the drying procedure required to conduct PXRD measurements induced phase transformations. To this end, COM crystals were suspended in ultrapure water, filtered, and dried without being exposed to isothermal dissolution experiments. The spectra belonging to these crystals exposed only to drying process, denoted as "COM in Water", share the identical peaks as the powder and COM reference. We can also conclude that drying process did not induce pseudopolymorphic/hydrate.

In addition to polymorphic form characterization in dissolution in ultrapure water, we also characterized the excess COM crystals from dissolution experiments at experimental pH values with Raman and PXRD (see Supplementary Materials). The PXRD and Raman spectra of excess crystals prior and after pH dependent solubility measurements were identical to COM patterns given in Figure 3 [58]. For brevity, we provide these spectra in the Supplementary Materials. We can conclude from our characterization, provided in Figure 3 and in Supplementary Materials, that isothermal dissolution experiments performed did not induce a detectable transition from COM to other CaOx hydrate forms. Naturally, we can only conclude that phase transition did not happen during our measurements within the accuracy of Raman and PXRD techniques. These techniques cannot detect pseudopolymorphic/hydrate below 5–10% by weight [59] hence we cannot entirely exclude possibility of phase transitions. We also explored techniques that offer single crystal level insights to potential transitions such as scanning electron microscopy, polarized light, and bright field microscopy (Supporting information). Yet it was difficult to visually identify CaOx hydrate morphologies from micrographs as most crystals were found as aggregates. We speculate this aggregation originates from capillary forces emerging in drying process [60]. In the light of these results, we only confirm no phase transitions occurred during solubility measurements within the accuracy of experimental techniques utilized in this study.

In Figure 4, the measured solubility of COM with ICP-OES at the four temperatures is given together with the simulated solubility values based on the literature values of the K values given in Table 3. The total calculated calcium ion concentration in the saturated solution using literature K_{sp} values from Streit et al. [22] are also shown (black stars) in Figure 4. It can be concluded that the use of these K_{sp} values results in a much lower solubility of COM compared to our measured values shown in

Figure 4. This is hardly surprising given the significant variations of the solubility data in the literature from which these K_{sp} values are estimated (Table 3).

To remove this discrepancy, we estimated new K_{sp} values for COM based on our measurements. We used the Van't Hoff equation given in Equation (5) to describe the temperature dependency of the K_{sp}.

Note that we cannot fit Equation (5) directly to the data of Figure 4, as we measure the total dissolved Ca ion concentration and the K_{sp} is expressed in terms of the activities of the free Ca^{2+} and $C_2O_4^{2-}$ ions. Therefore, we applied a parameter estimation procedure using the proposed model instead. To estimate the parameters in the Van't Hoff equation, $K_{sp,0}$ and ΔH_R where $K_{sp,0}$ is the solubility product of COM at standard conditions, simulations with the developed model were performed at the experimental temperatures. Then, the sum of the errors between the experimental and simulated total Ca^{2+} concentrations were calculated for a given parameter set. Finally, this error was minimized by variation of the two parameters numerically with a custom written code in Matlab.

Figure 4 shows the results of the parameter estimation comparing the experimental solubilities and the simulated values as a function of the temperature (pink solid line). Only the K_{sp} values were fitted, while the temperature dependence of the other K values for the protonation and dissociation constants were taken from the literature sources [33,47,49]. The results show an adequate fit of the experimental data using the parameters of 6.7×10^{-9} [mol^2/L^2] and 5.5 [kJ mol^{-1}] for the $K_{sp,0}$ and ΔH_R, respectively (see Table 3). The estimated K_{sp} values are somewhat higher than the ones reported in literature. Most literature values at 25 °C are at least a factor of two lower than our estimated K_{sp} value of 6.7×10^{-9} [mol^2/L^2]. The reported values are in the range from 1.77×10^{-9} to 2.85×10^{-9} [mol^2/L^2] [22,33,61]. This deviation stresses the need for a systematic comparison of the different methods to determine the solubility of such electrolyte crystallization systems with extreme low solubilities. We can only speculate that this variation might be due to experimental difficulties in measuring solubility of sparsely soluble salts such as COM or the presence of different pseudopolymorphic/hydrate, which we, to our best ability, monitor before and after dissolution experiments.

The total dissolved Ca^{2+} ion concentrations, measured using the ICP-OES method as a function of the pH at body temperature 37 °C in the presence two different buffer solutions are given in Figure 5. The experiments in the low pH range up to a pH of 7.55 were measured in the citric acid-disodium phosphate buffer (blue triangles), while the last two data points at the higher pH values, were measured in the glycine-sodium hydroxide buffer (blue circles).

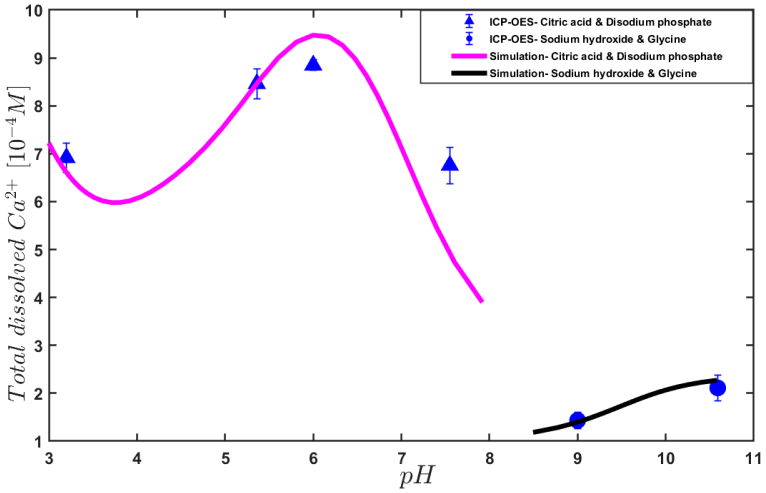

Figure 5. Total dissolved COM expressed as the total dissolved Calcium concentration in the solution citric acid-disodium phosphate buffer with a pH of 3.2, 5.36, 6.0, 7.55 (blue triangles) and glycine-sodium hydroxide buffer with a pH of 9.0, 10.6 (blue dots) at 37 °C. In addition, the simulated total dissolved Ca concentration as function of pH in a citric acid-disodium phosphate buffer (magenta line) and in a glycine-sodium hydroxide buffer (black line) is given.

The results show a large change in the total dissolved Ca^{2+} ion concentration as a function of the pH and a strong increase in the solubility compared to that in water, especially in the citric acid-disodium phosphate buffer.

The solution pH is observed to strongly influence the solubility of COM. A peak value of $8.847 \pm 0.112 \times 10^{-4}$ moles/L is found at a pH of 6.0 in a citric acid-disodium phosphate buffer, which is a factor of 8 higher than the one in ultrapure water at pH 7. In the glycine-sodium hydroxide buffer at pH 9.0 and 10.6, the solubility is much lower (between 1.43×10^{-4} M and 2.11×10^{-4} M at pH values of 9.0 and 10.6 respectively). Both towards lower and higher pH values the solubility drops to lower values. This is in accordance with results from medical studies showing a higher risk of formation of kidney stones pH values between 4.5 and 5.5 [8,18].

The theoretical model we developed explains this behavior. Our model suggests that the pH and the added buffer solution influence the ionic strength of the solution and consequently the solution chemistry and the speciation of the solution. Due to the increased ionic strength, the activity coefficients especially of the ions with high valence will decrease drastically reducing the activity and thus increasing the actual concentration at equilibrium.

Secondly, ion pair formation of calcium and oxalate ions with ions from the buffer solution can lower the free concentration of these ions in the solution considerably. Both effects will lead to a higher solubility of the COM in buffers compared to water. In the glycine-sodium hydroxide buffer solution at higher pH (at 9.0 and 10.6), the ionic strength is also high but apparently the ionic pair formations of the Calcium and Oxalate ions are much weaker than citric acid-disodium phosphate buffer.

In Figure 5, the pH dependence of the experimental and simulated total Calcium concentrations are also given (magenta and black solid lines denote simulations, circles and triangles denote experiments). As outlined before, the adapted values for the K_{sp} determined from the temperature dependent measurements in COM/water system were used in these simulations. The model predicts very well the observed measurements using the adapted K_{sp} value of 7.3×10^{-9} [mol^2/L^2], at 37 °C. In fact, the simulations results give an excellent match with the experimental results without any fudge factors, with a peak value of the solubility at pH 6 in the citric acid-disodium phosphate buffer. The lower total calcium ion concentrations at pH 3.2 compared to that at pH 7.55 in the citric acid- disodium phosphate buffer is described adequately. The prediction of the lower solubility of COM in the Glycine-Sodium hydroxide buffer by the model is also remarkable. Such remarkable prediction of the solubility in two different buffers from the solubility measurements of COM in pure water emphasizes the self-consistency of the proposed model and experimental procedure.

To explain the increased solubility of COM in the buffer solutions and its variation as a function of the pH we must have a closer look at the speciation calculated using the developed model. The simulation results given in Figures 6 and 7 explain the observed trends and shed light to the speciation in the system under study. In Figure 6a, the distribution of the Ca^{2+} species is shown as a function of pH in the citric acid-disodium phosphate buffer while Figure 6b shows the distribution of the $C_2O_4^{2-}$ in the same buffer. From Figure 6a, it can be seen that the fraction of free Ca^{2+} in solution is very small compared to the amount of Ca^{2+} ions bound at the citric acid complexes. Figure 6 also shows the strong variation of the relative amount of $CaCit^-$ and CaHCit as a function of pH as a result of the protonation reactions of the citric acid species. Concerning the oxalate species shown in Figure 6b, it is remarkable how high the free concentration becomes at pH values between 5 and 7. This is enabled by the deprotonation of the $HC_2O_4^-$ species and the low free Ca^{2+} concentration and the low activity of the Ca^{2+} and the $C_2O_4^{2-}$ ions in the high ionic strength of the buffer solutions. Comparison of panels a and b in Figure 6 also clearly shows that the stoichiometry of the free Ca^{2+} and $C_2O_4^{2-}$ varies strongly in the solution as a function of pH. A completely different ion speciation is observed in Figure 7 for calcium (panel a) and oxalate (panel b) ions in glycine-sodium hydroxide buffer at the same temperature. Figure 7 shows that in the glycine-sodium hydroxide buffer, a considerable portion of total calcium ions is free Ca^{2+} in solution. The relative amount of free Ca^{2+} decreases with increasing pH significantly by the formation of $CaGly^+$ complexes. In the glycine-sodium hydroxide

buffer, almost all the oxalate consists of free $C_2O_4^{2-}$ ions over the entire pH range as is shown in Figure 7b. Apparently, the speciation of the oxalate is not much affected by complex formation in this solution; the increase in the solubility with respect to that in pure water is caused by the ionic strength of the solution.

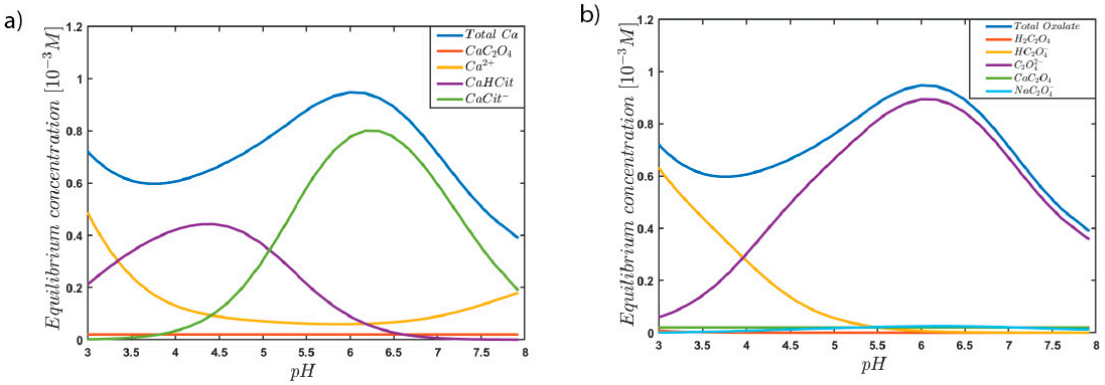

Figure 6. Simulated equilibrium concentrations of the Calcium (**a**) and the oxalate (**b**) species at various pH in citric acid-disodium phosphate buffer at 37 °C.

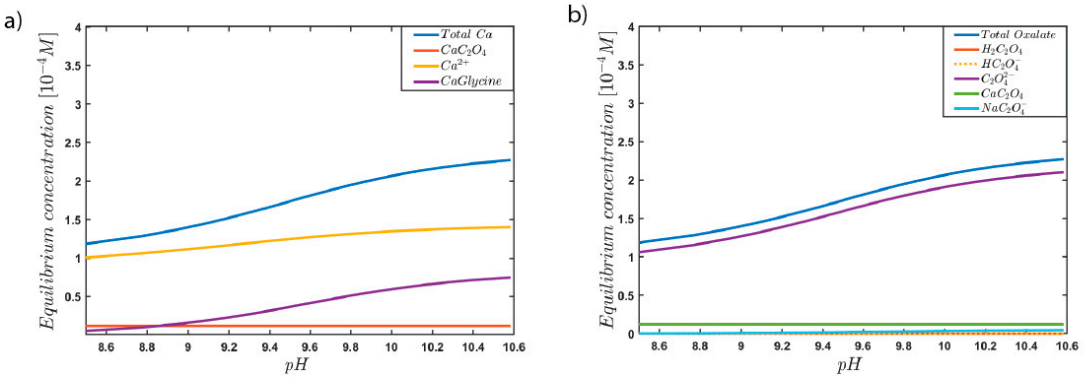

Figure 7. Simulated distribution of the calcium (**a**) and the oxalate (**b**) species at various pH in citric acid-disodium phosphate buffer at 37 °C.

4. Conclusions

The reported solubility values of COM in ultrapure water vary significantly depending on the source and technique evoked in literature. To shed light on the origin of this variability and to establish a self-consistent methodology, we present a cross-validated experimental and modelling study of solubility of COM as a function of temperature and pH while carefully monitoring potential phase transitions.

In this study, the measured solubility of COM in ultrapure water at room temperature is higher than majority of literature values [24–26,28], yet some studies report even higher values than our measurements. We discuss the origin of this variation and speculate that it might arise from experimental challenges, particularly subjectivity in manual methods such as titration, impurity incorporation, and potential pseudopolymorphic/hydrate transitions. Our experimental results indicate that solubility of COM has only modest temperature dependence, in agreement with earlier measurements [19,26]. We estimated K_{sp} values from measured solubilities as a function of temperature using the Van't Hoff equation and the proposed model. Parameter estimation of the Van't Hoff equation is performed minimizing the error between the simulated and the measured solubility of COM in ultrapure water at different temperatures to estimate K_{sp} values. The resulting parameters for the Van't Hoff equation are estimated to be 6.7×10^{-9} [mol^2/L^2] and 5.5 [J mol^{-1}] for $K_{sp,0}$ and ΔH_R, respectively. Using these parameters, the developed model not only describes the temperature dependent solubilities in

ultrapure water, but also permits the prediction of the pH dependent measurements in buffer solutions at body temperature.

The solubility of COM as a function of pH measured at body temperature in two different buffer solutions showed a strong dependence of the solubility on the pH with an eightfold increased solubility around a pH of 6 in a citric acid-disodium phosphate buffer compared to that of COM in ultrapure water. The proposed model enabled the interpretation of this enhanced solubility of COM in buffer solutions as the combined effect of increased ionic strength, protonation reactions and soluble complex formation. Moreover, the developed model estimates the solubility in the two separate buffer solutions remarkably well using K_{sp} values extracted from the measurements in ultrapure water without any fudge factors, highlighting the self-consistency of our approach. The presented combined experimental and modelling study establishes a firm basis to extend the physiochemical understanding of nephrolithiasis to more complex biological solutions.

Supplementary Materials: The following are available online at http://www.mdpi.com/2073-4352/10/10/0924/s1. A combined study and modelling of Solubility of Calcium Oxalate Monohydrate at physiologically relevant pH and temperatures have been elaborated.

Author Contributions: The manuscript was written through contributions of all authors. All authors have read and agreed to the published version of the manuscript.

Funding: F.I. acknowledges financial support from the Scientific and Technological Research Council of Turkey (TUBITAK), Grant No: 2213. H.B.E. acknowledges the Netherlands Organization for Scientific Research (NWO) for financial support through Veni grants (project numbers 722-014-007).

Acknowledgments: Authors would like to thank Michel van den Brink for his valuable help in ICP-OES measurement.

Conflicts of Interest: The authors declare no conflict of interest.

Abbreviations

ICP-OES	Inductively coupled plasma optical emission spectrometry,
ICP-MS	Inductively coupled plasma mass spectrometry,
FBRM	Focused beam reflectance measurement,
UV-VIS	Ultraviolet–visible spectrophotometry,
COM	Calcium oxalate monohydrate,
CaOx	Calcium oxalate,
AAS	Atomic absorption spectrophotometers.

References

1. Alelign, T.; Petros, B. Kidney stone disease: An update on current concepts. *Adv. Urol.* **2018**, *2018*, 1–12. [CrossRef]
2. Bowers, G.M.; Kirkpatrick, R.J. Natural Abundance43Ca NMR as a tool for exploring calcium biomineralization: Renal stone formation and growth. *Cryst. Growth Des.* **2011**, *11*, 5188–5191. [CrossRef]
3. Goldfarb, D.S. A woman with recurrent calcium phosphate kidney stones. *Clin. J. Am. Soc. Nephrol.* **2012**, *7*, 1172–1178. [CrossRef]
4. Zhai, H.; Wang, L.; Putnis, C.V. Inhibition of spiral growth and dissolution at the brushite (010) interface by chondroitin 4-sulfate. *J. Phys. Chem. B* **2019**, *123*, 845–851. [CrossRef]
5. Worcester, M.E.; Coe, F.L. Nephrolithiasis. *Prim. Care Clin. Off. Pract.* **2008**, *35*, 369–391. [CrossRef]
6. Maarten, T.; Glenn, C.; Philip, M.; Karl, S.; Alan., Y.; Barry, B. *Brenner and Rector's the Kidney E-Book*; Elsevier Health Sciences: Amsterdam, The Netherlands, 2015.
7. Romero, V.; Akpinar, H.; Assimos, D.G. Kidney stones: A global picture of prevalence, incidence, and associated risk factors. *Rev. Urol.* **2010**, *12*, e86–e96. [PubMed]
8. Ridley, J.W. *Fundamentals of the Study of Urine and Body Fluids*; Springer: Berlin/Heidelberg, Germany, 2018.
9. Bird, V.Y.; Khan, S.R. How do stones form? Is unification of theories on stone formation possible? *Arch. Españoles Urol. (Ed. Impresa)* **2017**, *70*, 12–27.

10. Hall, V.M.; Thornton, A.; Miehls, E.K.; Bertke, J.A.; Swift, J.A. Uric acid crystallization interrupted with competing binding agents. *Cryst. Growth Des.* **2019**, *19*, 7363–7371. [CrossRef]
11. Khan, S.R.; Pearle, M.S.; Robertson, W.G.; Gambaro, G.; Canales, B.K.; Doizi, S.; Traxer, O.; Tiselius, H.-G. Kidney stones. *Nat. Rev. Dis. Prim.* **2016**, *2*, 16009. [CrossRef]
12. Miller, G.; Vermeulen, C.; Moore, J. Calcium oxalate solubility in urine: Experimental urolithiasis XIV. *J. Urol.* **1958**, *79*, 607–612. [CrossRef]
13. Izatulina, A.R.; Gurzhiy, V.V.; Krzhizhanovskaya, M.; Kuz'Mina, M.A.; Leoni, M.; Frank-Kamenetskaya, O.V. Hydrated calcium oxalates: crystal structures, thermal stability, and phase evolution. *Cryst. Growth Des.* **2018**, *18*, 5465–5478. [CrossRef]
14. Kelland, M.A.; Mady, M.F.; Lima-Eriksen, R. Kidney stone prevention: dynamic testing of edible calcium oxalate scale inhibitors. *Cryst. Growth Des.* **2018**, *18*, 7441–7450. [CrossRef]
15. Pahira, J.J.; Pevzner, M. Nephrolithiasis. In *Penn Clinical Manual of Urology*; Elsevier: Amsterdam, The Netherlands, 2007; pp. 235–257.
16. Sun, X.-Y.; Zhang, C.-Y.; Bhadja, P.; Ouyang, J.M. Preparation, properties, formation mechanisms, and cytotoxicity of calcium oxalate monohydrate with various morphologies. *CrystEngComm* **2018**, *20*, 75–87. [CrossRef]
17. Worcester, E.M.; Coe, F.L. Calcium kidney stones. *N. Engl. J. Med.* **2010**, *363*, 954–963. [CrossRef] [PubMed]
18. Childs-Sanford, S. The captive maned wolf (Chrysocyon brachyurus): nutritional considerations with emphasis on management of cystinuria. In *Proceedings of the Fourth Conference on Zoo and Wildlife Nutrition*; Edwards, M., Lisi, K.J., Schlegel, M.L., Bray, R.E., Eds.; AZA Nutrition Advisory Group: Lake Buena Vista, FL, USA, 2005.
19. Bono, M.J.; Reygaert, W.C. Urinary Tract Infection. In *StatPearls*; StatPearls Publishing: Treasure Island, FL, USA; Available online: https://www.ncbi.nlm.nih.gov/books/NBK470195/ (accessed on 12 October 2020).
20. Singh, R.P. On the existence of $NaC_2O_4^-$ ion pair complex. *Bull. Chem. Soc. Jpn.* **1989**, *62*, 4089–4091. [CrossRef]
21. Pan, H.-B.; Darvell, B.W. Calcium phosphate solubility: The need for re-evaluation. *Cryst. Growth Des.* **2009**, *9*, 639–645. [CrossRef]
22. Streit, J.; Tran-Ho, L.-C.; Königsberger, E. Solubility of the three calcium oxalate hydrates in sodium chloride solutionsand urine-like liquors. *Mon. Chem. Chem. Mon.* **1998**, *129*, 1225–1236. [CrossRef]
23. Molzon, J.A. The Solubility of Calcium Oxalate as a Function of Dielectric Constant. Master's Thesis, University of Rhode Island, Kingston, RI, USA, 1976.
24. McComas, W.H., Jr.; Rieman, W. The Solubility of calcium oxalate monohydrate in pure water and various neutral salt solutions at 25. *J. Am. Chem. Soc.* **1942**, *64*, 2946–2947. [CrossRef]
25. Shehyn, H.; Pall, D.B. The solubility of calcium oxalate in various salt solutions. *J. Phys. Chem.* **1940**, *44*, 166–171. [CrossRef]
26. Gutzow, I.; Atanassova, S.; Budevsky, G.; Neykov, K. Solubility, inhibited growth and dissolution kinetics of calcium oxalate crystals in solutions, containing hippuric acid. *Urol. Res.* **1993**, *21*, 181–185. [CrossRef]
27. Muhs, G.; Herz, W. Ueber die Lösliohkeit einiger Salze der Ekdalkalimetalle mit organisohen Sauren in Essigsiiure. *Ber. Dtsch. Chem. Ges.* **1903**, *36*, 3715–3718.
28. Hammersten, G. *On Calcium Oxalate and Its Solubility in the Presence of Inorganic Salts with Special Reference to the Occurrence of Oxaluria*; C.R. Trav. Lab. Carlsberg: Copenhagen, Denmark, 1929; Volume 17, p. 1.
29. Gardner, G.L.; Nancollas, G.H. Kinetics of dissolution of calcium oxalate monohydrate. *J. Phys. Chem.* **1975**, *79*, 2597–2600. [CrossRef]
30. Robertson, W.G. Diet and calcium stones. *Miner. Electrolyte Metab.* **1987**, *13*, 228–234. [PubMed]
31. Finlayson, B.; Roth, R. Appraisal of calcium oxalate solubility In sodium chloride and sodium-calcium chloride solutions. *Urology* **1973**, *1*, 142–144. [CrossRef]
32. Gardner, G.L.; Nancollas, G.H. Crystal growth in aqueous solution at elevated temperatures. Barium sulfate growth kinetics. *J. Phys. Chem.* **1983**, *87*, 4699–4703. [CrossRef]
33. Garside, J.; Brečević, L.; Mullin, J. The effect of temperature on the precipitation of calcium oxalate. *J. Cryst. Growth* **1982**, *57*, 233–240. [CrossRef]
34. Baumann, J.; Ackermann, D.; Affolter, B. The influence of hydroxyapatite and pyrophosphate on the formation product of calcium oxalate at different pHs. *Urol. Res.* **1989**, *17*, 153–155. [CrossRef]

35. Tiselius, H.-G. The effect of ph on the urinary inhibition of calcium oxalate crystal growth. *BJU Int.* **1981**, *53*, 470–474. [CrossRef]
36. Højgaard, I.; Fornander, A.-M.; Nilsson, M.-A.; Tiselius, H.-G. The effect of pH changes on the crystallization of calcium salts in solutions with an ion composition corresponding to that in the distal tubule. *Urol. Res.* **1999**, *27*, 409–416. [CrossRef]
37. Elemental-Analysis/icp-ms. Available online: https://www.ru.nl/science/gi/facilities-activities/ (accessed on 15 January 2019).
38. Elemental-Analysis/icp-oes. Available online: https://www.ru.nl/science/gi/facilities-activities/ (accessed on 15 February 2019).
39. Elkadi, M.; Ae, P.; Fok, S.; Feghali, F.; Bassioni, G.; Stephen, S. Depth profiling (ICP-MS) study of toxic metal buildup in concrete matrices: Potential environmental impact. *Sustainability* **2010**, *2*, 3258–3269. [CrossRef]
40. Biological-Buffers/Learning-Center/Buffer-Reference-Center.html, Sigma-Aldrich. Buffer Reference Center. Available online: https://www.sigmaaldrich.com/life-science/core-bioreagents/ (accessed on 15 May 2019).
41. Buffers, Plant Microtechnique and Microscopy. 1999. Available online: http://microscopy.berkeley.edu/Resources/instruction/buffers.html (accessed on 15 May 2019).
42. Vallapragada, V.V.; Inti, G.; Ramulu, J. A validated inductively coupled plasma-optical emission spectrometry (ICP-OES) method to estimate free calcium and phosphorus in in vitro phosphate binding study of eliphos tablets. *Am. J. Anal. Chem.* **2011**, *2*, 718–725. [CrossRef]
43. Green, D.R.H.; Cooper, M.J.; German, C.R.; Wilson, P.A. Optimization of an inductively coupled plasma-optical emission spectrometry method for the rapid determination of high-precision Mg/Ca and Sr/Ca in foraminiferal calcite. *Geochem. Geophys. Geosyst.* **2003**, *4*. [CrossRef]
44. De Souza, R.M.; Leocádio, L.G.; Da Silveira, C.L.P. ICP OES simultaneous determination of Ca, Cu, Fe, Mg, Mn, Na, and P in biodiesel by axial and radial inductively coupled plasma-optical emission spectrometry. *Anal. Lett.* **2008**, *41*, 1615–1622. [CrossRef]
45. Buffer. Available online: https://www.sigmaaldrich.com/life-science/core-bioreagents/biological-buffers/learning-center/buffer-reference-center.html#citric2 (accessed on 15 June 2019).
46. Nancollas, G.; Gardner, G. Kinetics of crystal growth of calcium oxalate monohydrate. *J. Cryst. Growth* **1974**, *21*, 267–276. [CrossRef]
47. Singh, R.P.; Yeboah, Y.D.; Pambid, E.R.; Debayle, P. Stability constant of the calcium-citrate(3-) ion pair complex. *J. Chem. Eng. Data* **1991**, *36*, 52–54. [CrossRef]
48. May, P.M.; Murray, K.; Williams, D.R. The use of glass electrodes for the determination of formation constants—II Simulation of titration data. *Talanta* **1985**, *32*, 483–489. [CrossRef]
49. Davies, C.W.; Hoyle, B.E. 842. The interaction of calcium ions with some phosphate and citrate buffers. *J. Chem. Soc.* **1953**, 4134. [CrossRef]
50. Robertson, W. Measurement of ionized calcium in biological fluids. *Clin. Chim. Acta* **1969**, *24*, 149–157. [CrossRef]
51. Marrero, V.R.V.; Berríos, C.P.; Rodríguez, L.D.D.; Stelzer, T.; López-Mejías, V. In the context of polymorphism: Accurate measurement, and validation of solubility data. *Cryst. Growth Des.* **2019**, *19*, 4101–4108. [CrossRef]
52. Richards, T.W.; Zeitschr, C.T.M.a.H.B. Anorg. Chemie. 1901. 28. Available online: https://books.google.nl/books?id=wu1FmlWKW_MC&pg=PA101&lpg=PA101&dq=Richards,+proc.+am.+acad.+arts+sci+36+375+1901&source=bl&ots=KsxL2v70ll&sig=ACfU3U0s4_EImd7LHcR9pswRqXwpwBEfcg&hl=en&sa=X&ved=2ahUKEwi51bKuqdzjAhWIJFAKHbVdC5wQ6AEwAHoECAkQAQ#v=onepage&q=Richards%2C%20proc.%20am.%20acad.%20arts%20sci%2036%20375%201901&f=false (accessed on 15 June 2018).
53. Hall, W.T. The oxalate method for separating calcium and magnesium. *J. Am. Chem. Soc.* **1928**, *50*, 2704–2707. [CrossRef]
54. Frausto-Reyes, C.; Loza-Cornejo, S.; Terrazas, T.; Miranda-Beltrán, M.D.L.L.; Aparicio-Fernández, X.; López-Macías, B.M.; Morales-Martínez, S.E.; Ortiz-Morales, M. Raman spectroscopy study of calcium oxalate extracted from cacti stems. *Appl. Spectrosc.* **2014**, *68*, 1260–1265. [CrossRef] [PubMed]
55. Kodati, V.R.; Tomasi, G.E.; Turumin, J.L.; Tu, A.T. Raman spectroscopic identification of calcium-oxalate-type kidney stone. *Appl. Spectrosc.* **1990**, *44*, 1408–1411. [CrossRef]
56. Edwards, H.G.M.; Seaward, M.R.D.; Attwood, S.J.; Little, S.J.; De Oliveira, L.F.C.; Tretiach, M. FT-Raman spectroscopy of lichens on dolomitic rocks: an assessment of metal oxalate formation. *Analyst* **2003**, *128*, 1218–1221. [CrossRef] [PubMed]

57. Orlando, M.T.D.; Kuplich, L.; De Souza, D.O.; Belich, H.; Depianti, J.B.; Orlando, C.G.P.; Medeiros, E.F.; Da Cruz, P.C.M.; Martinez, L.G.; Corrêa, H.P.S.; et al. Study of calcium oxalate monohydrate of kidney stones by X-ray diffraction. *Powder Diff.* **2008**, *23*, S59–S64. [CrossRef]
58. Manzoor, M.A.P.; Agrawal, A.K.; Singh, B.; Mujeeburahiman, M.; Rekha, P.D. Morphological characteristics and microstructure of kidney stones using synchrotron radiation μCT reveal the mechanism of crystal growth and aggregation in mixed stones. *PLoS ONE* **2019**, *14*, e0214003. [CrossRef] [PubMed]
59. Hammond, R.; Pencheva, K.; Roberts, K. Molecular modeling of crystal−crystal interactions between the α-and β-polymorphic forms of l-glutamic acid using grid-based methods. *Cryst. Growth Des.* **2007**, *7*, 875–884. [CrossRef]
60. Eral, H.B.; O'Mahony, M.; Shaw, R.; Trout, B.L.; Myerson, A.S.; Doyle, P.S. Composite hydrogels laden with crystalline active pharmaceutical ingredients of controlled size and loading. *Chem. Mater.* **2014**, *26*, 6213–6220. [CrossRef]
61. Blomen, L.J.; Will, E.J.; Bijvoet, O.L.; Van Der Linden, H. Growth kinetics of calcium oxalate monohydrate: II. The variation of seed concentration. *J. Cryst. Growth* **1983**, *64*, 306–315. [CrossRef]